Back to Session Subjects

NUMERICAL SIMULATION RESULTS OF THE MAIN ROTOR AERODYNAMICS

Viktor A. Anikin, Dmitry S. Kolomenskiy

KAMOV Company, Russia

Key words: Rotor aerodynamics, numerical simulation

Abstract: The paper discusses problems of numerical simulation of high-speed maneuverable helicopter rotor aerodynamics.

The effects of
- spatial airflow about the main rotor blades;
- development of vortices in the reverse flow region;
- unsteady nature of the distributed and integral aerodynamic coefficients of the rotor;
- induction in rotor systems, in particular coaxial rotors

are considered in the context of a new-developed mathematical model, which is based on the time-accurate non-linear vortex theory.

Numerical analysis results of the main rotor forces and moments are presented for high flight speeds and g-loads. A comparison of calculated and experimental results for a large-scale main rotor model is given.

1 PROBLEM DEFINITION. MATHEMATICAL MODEL OF THE MAIN ROTOR AERODYNAMICS

The problem definition was stated in [3, 4]. In this paper only the main points of the developed mathematical model are highlighted.

The mathematical model consists in a consecutive time-accurate solution of two problems.

<u>The first problem</u> represents determination of vortical intensity distribution along the blades and the induced velocity field, which is done in the context of the inviscid fluid. The time-accurate non-linear vortex theory [2, 6] is used for these purposes.

It considers a rotor in 3-D transient motion. Its blades are substituted by thin lifting surfaces S_i, the airflow over which may separate from the trailing and side edges and partly from the leading edges (Fig. 1).

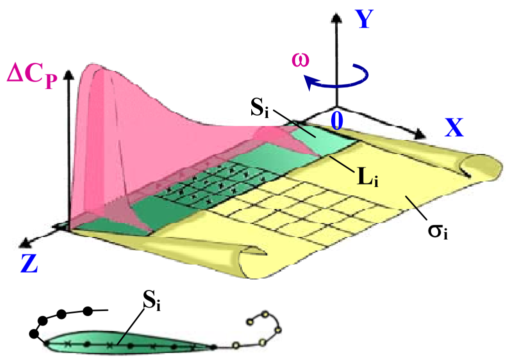

Figure 1.

The airflow about the rotor generates a developed vortical wake in the form of vortex sheets σ_i.

Improvements in describing the vortex shed of the reverse flow region are introduced. Two models of the blade aerodynamics in the reverse flow region are proposed. In the “attached” model vortex sheets are generated in accordance with Fig. 2. In the “stalled” model vortex sheets are generated in accordance with Fig. 3.

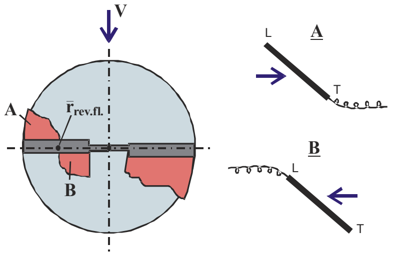

Figure 2.

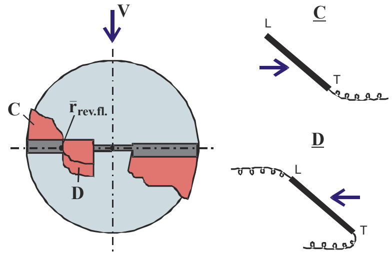

Figure 3.

A boundary problem is formulated to determine a velocity potential function satisfying Laplace equation and the corresponding boundary conditions.

Numerical realization of the boundary problem represents space-time discretization using discrete vortex method. As a result a system of linear algebraic equations governing the intensities of the attached vortex filaments is obtained at each time step. The solution of this system gives the required intensities and the induced velocity field.

<u>The second problem</u> is the determination of the main rotor forces and moments. It implements the traditional approach [1] of summing-up elementary forces and moments at all blade sections, which take into account the effects of viscosity and density of the fluid. In addition to the traditional approach the transient effects are also present.

Introducing the angle of attack concept in the lifting surface theory allows associating blade section forces and moments with forces and moments of an infinite-span wing in level motion, slipping, in the general case. This uses the induced velocities determined by solving the first problem. Blade section induced angle of attack represents an integral estimate of chordwise distributed local angle of attack, which may be defined in a number of ways.

One of the possible approaches is to determine true angles of attack in control points located at the distance of 1/4 chord from the leading edge, the same as in the lifting line theory. Methodological studies and comparison with the experimental data have proven this method to be not fully satisfactory when used in the context of the lifting surface theory and have shown it to overestimate the blade lift.

In the method of «3/4» true angles of attack are determined from the components of the inflow velocity V calculated in control points at the distance of z=3/4 chord from the leading edge.

In [5] there was proposed a way to implement the flat section hypothesis within the lifting surface theory, which uses an assumption that sectional normal forces of the blade and of an infinite-span wing must be equal.

The latter two methods give close results for the main rotor blades (aspect ratio $\lambda \geq 10$, see Fig. 4).

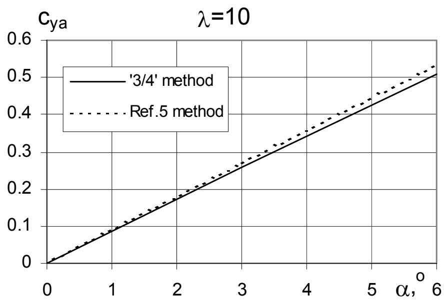

Figure 4.

With an increase in the advance ratio over $\overline{V}$ =0.4 radial flows along the blades remarkably grow and spatial airflow effects must be taken into account. Using the traditional hypothesis of flat sections normal to the blade axis results in considerable errors.

A hypothesis of skewed sections arranged under varied slip angles along the blade is introduced (Fig. 5): the forces acting on a lifting surface element in 3D flow are equal to the forces acting on the same element acting in 2D flow with appropriate flow velocity and angles of slip and attack

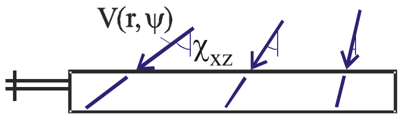

Figure 5.

By the way of building a section along the streamline under a certain angle to the blade axis we obtain other airfoils differing from those normal-section profiles that make the blade. Situation becomes more complicated when the blade is twisted and/or it consists of different airfoils.

An infinite-span swept wing with χ_{xz} sweepback at quarter chord is schemed based on the skewed section profile.

There were developed two versions of calculation procedure to determine aerodynamic coefficients of a wing using the skewed section hypothesis. The first version assumes calculation of slipping infinite-span wing aerodynamic coefficients. It is used when slipping is modeled by the method of calculating airfoil forces and moment. The second variant based on the superposition principle appeals to an infinite-span wing with the flow velocity normal to its axis. The equivalence of the above variants is proved theoretically as well as by the comparative calculations of the high aspect ratio slipping and non-slipping wings using 3D Euler.

Aerodynamic coefficients of the obtained infinite-span wing are calculated using an airfoil aerodynamics program package, with its components specialized in calculating airfoil aerodynamic coefficients under different conditions of the airflow. It is composed of the recognized models and programs tested on typical helicopter airfoils. Each section corresponds with one of the airfoil aerodynamics models according to the section angle of attack, Mach, Reynolds and Strouhal numbers:
- calculation of airfoil aerodynamics in a transsonic flow;
- calculation of airfoil aerodynamics in a subsonic flow with moderate Reynolds numbers;
- calculation of airfoil unsteady aerodynamics;
- interpolation of experimental forces and moments.

The method used to calculate aerodynamic coefficients of each section is selected so as to fulfill robustness and validity conditions of the airfoil subprograms, which have been evaluated by an analysis based on some typical helicopter airfoil forces and moment computation. It is also possible to use a combined method which utilizes experimental data obtained in wind tunnels.

Summing-up aerodynamic forces and moments of all the blade elements results in aerodynamic forces and moments of the rotor.

Thus the developed mathematical model enables calculation of rotor aerodynamic coefficients within a wide range of its operation conditions.

2 INFLUENCE OF SPATIAL AIRFLOW ABOUT THE BLADES ON THE MAIN ROTOR AERODYNAMIC COEFFICIENTS

Comparative analysis of the main rotor forces and moments using the skewed section hypothesis and the hypothesis of flat sections perpendicular to the blade axis was carried out to investigate the influence of spatial airflow about the main rotor blades on its aerodynamic coefficients.

High advance ratios of flight were considered: $\overline{V}$=0.4, 0.55 and 0.7.

As an example we shall demonstrate the spatial airflow influence on the rotor torque coefficient. Fig. 6 shows the difference in calculated torque coefficient as a function of increasing advance ratio:

$$\Delta = \left| \frac{(m_k/\sigma)_{skew} - (m_k/\sigma)_{norm}}{(m_k/\sigma)_{skew}} \right|,$$

where $(m_k/\sigma)_{skew}$ is calculated using the skewed section hypothesis and $(m_k/\sigma)_{norm}$ is calculated using the hypothesis of flat sections perpendicular to the blade axis.

The value of Δ increases with the increase in advance ratio from 2% at $\overline{V}$ = 0.4 up to 9% at $\overline{V}$=0.7.

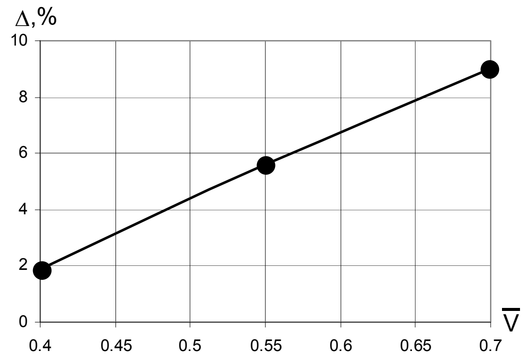

Figure 6.

The other aerodynamic coefficients are influenced in the similar way.

The obtained results demonstrate the noticeable influence of spatial airflow about the main rotor blades on its aerodynamic coefficients at high advance ratio $\overline{V}$>0.4.

3 INFLUENCE OF FLOW SEPARATION IN THE REVERSE FLOW REGION ON MAIN ROTOR AERODYNAMIC COEFFICIENTS

The influence of the reverse flow region on the rotor integral and distributed forces and moments is investigated by the example of a single-bladed rigid rotor. Consider the following operating conditions: $\overline{V}$ =0.7, α_R=-20°.

In these conditions the reverse flow region is large, airflow about the blade in this region has the strong influence on the rotor aerodynamic coefficients.

Fig. 7 shows normal force per unit length as a function of blade non-dimensional radius at the azimuth angles ψ=0, 90°, 180° и 270°:

$$\overline{Y}_{sec} = \frac{Y_{sec}}{0.5\rho(\omega R)^2 b},$$

where Y_{sec} is the non-dimensional normal to chord aerodynamic force of a section with radius $\overline{r}$; ω - rotor rotational speed, m/s; R – rotor radius, m; b – blade section chord, m; ρ - fluid (air) density, kg m^{-3}.

The fact of taking into account the reverse flow leads to higher negative thrust of root sections at the azimuth angles near ψ=270°. For the "stalled" model it is smaller than for the "attached", which is generally typical for the developed stall.

It is also necessary to note significant influence of the root vortex sheet. Taking account of the root vortex sheet results in smoother distribution of the blade root airloads at ψ=180°…270° (Fig. 7 c-d).

Fig. 8 shows the reverse flow region vortex shed ("stalled" model) as it develops in time. Blade root enters the reverse flow region as soon as at the azimuth angle ψ=210°. At ψ=210°…270° stall develops up to non-dimensional radius $\overline{r} = 0.7$. A vortex sheet generated by the leading edge separation is located downstream from the rotor, and it is mainly self-induced velocities that cause its deformation.

At ψ=270°…295° a tip vortex approaches the root of the blade, passes by it, and at ψ=345° it reaches the tip. At this azimuth the vortex sheet generated by the reverse flow region is also located near the blade tip. Such position of the vortex shed in some operation conditions can cause strong oscillation of blade airloads at ψ=270°…0.

As the presented results demonstrate, the blade stall in the reverse flow region has a significant influence on the main rotor aerodynamic forces at high advance ratios. It is particularly important to model the reverse flow region stall when dealing with the problems where distributed airloads represent the main point of interest.

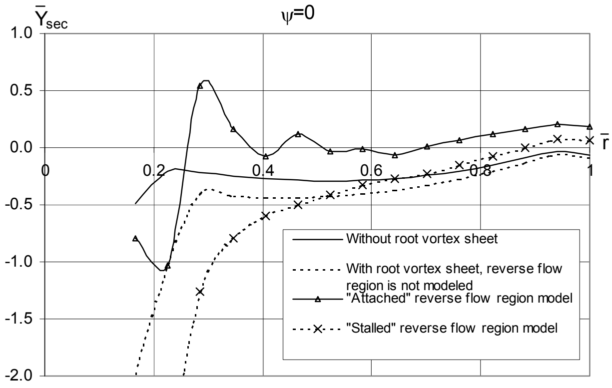

a)

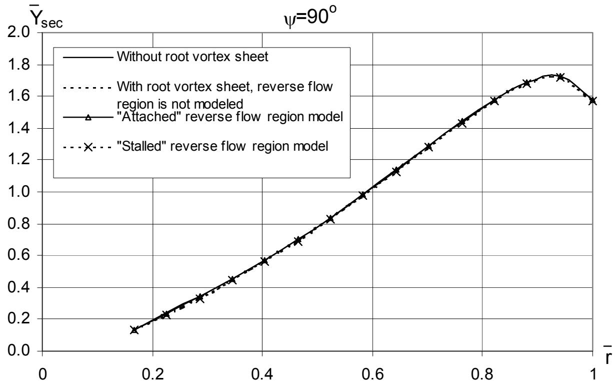

b)

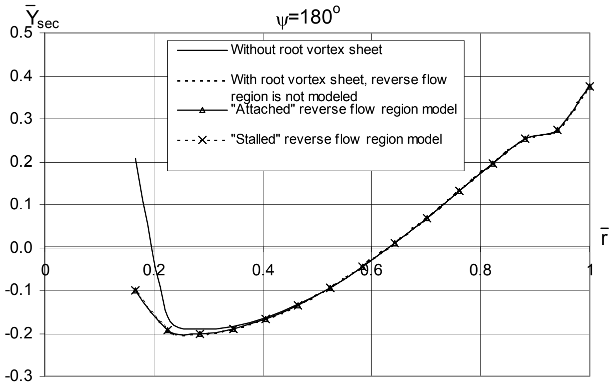

c)

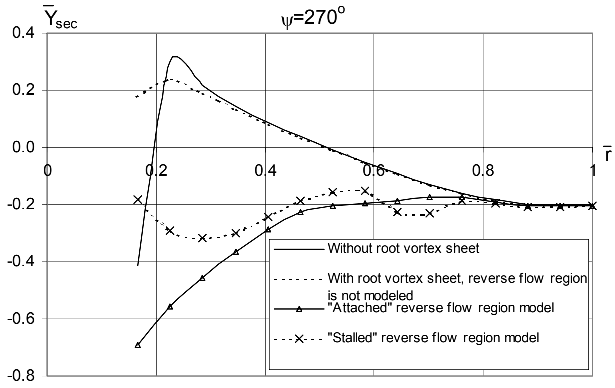

d)

Figure 7.

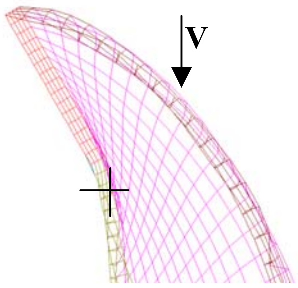

a) ψ=210°

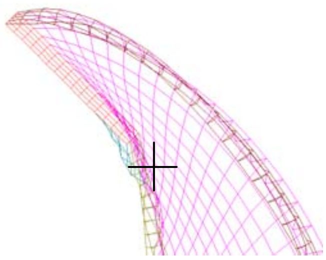

b) ψ=225°

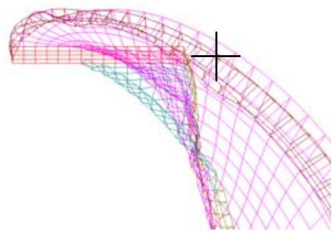

c) ψ=270°

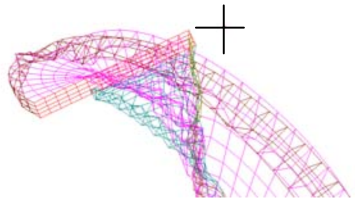

d) ψ=295°

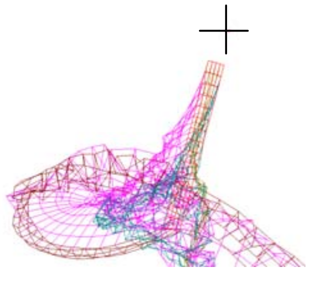

e) ψ=345°

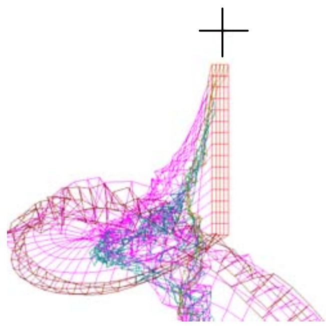

f) ψ=360°

Figure 8.

4 INDUCTION

The mathematical model allows investigating interactions of the vortex shed with the rotor blades, their average as well as distributed airloads. Rotor disk-averaged induced velocity decreases with increasing flight speed. However, at high advance ratio the rotor vortex shed becomes more nonuniform, which causes significant perturbation of the blade loads when it crosses the intensive vortices (see Fig. 9, where $\overline{\Gamma}$ is non-dimensional per unit length attached circulation). In these conditions vortices generated by the blade root and reverse flow region also have a considerable influence.

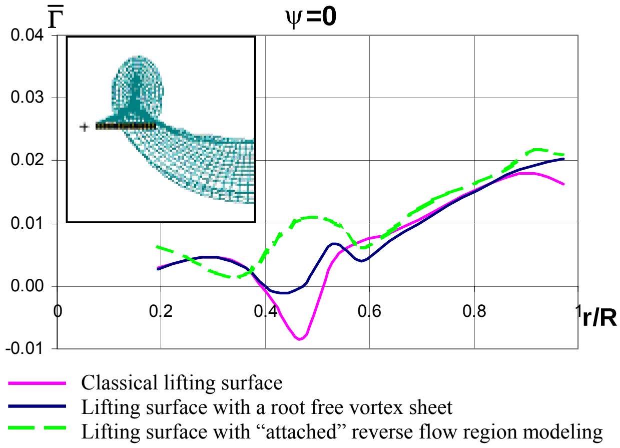

Figure 9.

5 COAXIAL ROTORS

More complex interactions are observed for the lower coaxial rotor blades and vortices off the upper rotor. Fig. 10 shows the change of higher and lower coaxial rotors thrust coefficients c_T in azimuth.

Average thrust coefficient c_{T0} of the upper rotor is higher than of the lower one, and the amplitude of its time-dependent part Δc_T is smaller. This confirms the known results. With an increase in advance ratio up to $\overline{V}$=0.2 the upper and the lower rotor thrust become close (Fig. 11).

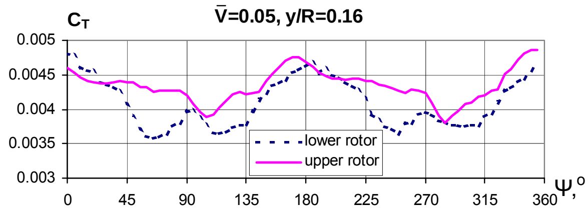

Figure 10.

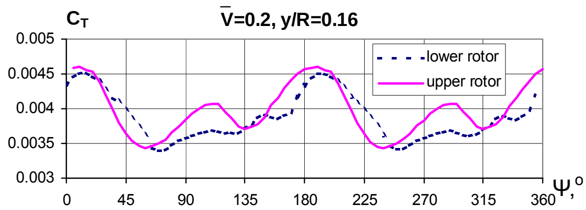

Figure 11.

Fig. 12 illustrates the lower rotor interaction with the vortex wake of the higher rotor at $\overline{V}$=0.2. Higher rotor blade tip vortices approach near to a lower rotor blade at ψ=0, and are deformed as a result of the induced interaction.

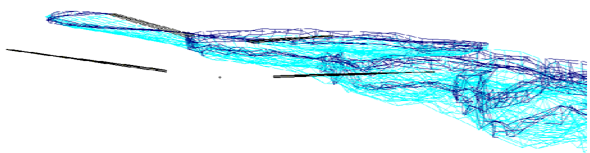

Figure 12.

Fig. 13 shows distribution of c_y along the lower blade, calculated using discretization levels of 7 and 14 vortex cells along the blade radius. As the obtained results confirm, even a coarse discretization provides accuracy acceptable for practical applications.

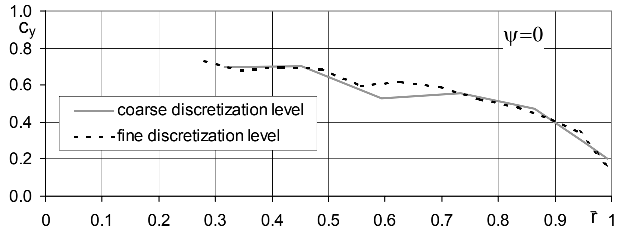

Figure 13.

6 TIME-DEPENDENT VARIATION OF AERODYNAMIC FORCES AND MOMENTS

Taking account of the transitional effects and vortex interactions makes the developed model suitable for investigation of various factors that influence the time-dependent part of the rotor forces and moments.

Aerodynamic coefficients of coaxial rotors with varied number of blades z_b and constant solidity σ=0.0576 have been calculated. Rotors phase angle $\Delta\psi^*$, i.e. azimuth angle of the upper rotor at zero azimuth of the lower rotor, has been varied. Relative distance between the rotors is assumed to be y/R=0.16, with an exception of the case when the distance has been increased to y/R=1. The calculations are made for constant thrust and drag.
Now consider the influence of the above design parameters on the rotor operating at $\overline{V}$=0.2, $\alpha_в$=-9°.

Fig. 14 shows function $c_т(\psi)$ of a coaxial rotor with z_b=2×2 (the first number is for rotors, the second is for blades of each rotor) for various $\Delta\psi^*$. Behavior of $c_т(\psi)$ significantly changes with the variation of $\Delta\psi^*$. As it is seen from Fig. 15, Δc_T maximizes when $\Delta\psi^*$=0…30°. Minimum of Δc_T corresponds to $\Delta\psi^*$=120° for z_b=2×2 and $\Delta\psi^*$=60° for z_b=2×3.

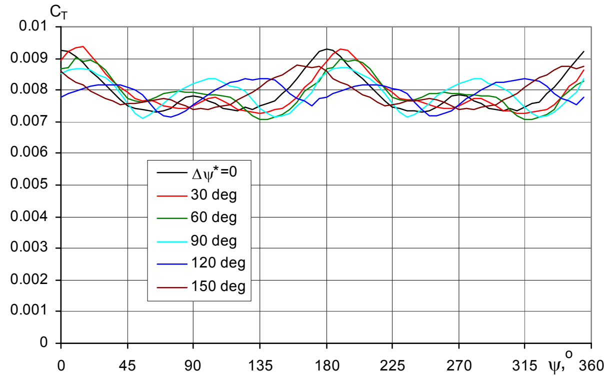

Figure 14.

Fig. 15-18 use the following nomenclature to designate relative amplitude of the time-dependent part of aerodynamic coefficients c_T, c_H, c_S и m_K:

$$\Delta\overline{c}_{\mathrm{T}} = \frac{\Delta c_{\mathrm{T}}}{c_{\mathrm{T}0}},\quad \Delta c_{\mathrm{T}} = \max(c_{\mathrm{T}}) - \min(c_{\mathrm{T}}),$$

$$\Delta\overline{c}_{\mathrm{H}} = \frac{\Delta c_{\mathrm{H}}}{c_{\mathrm{T}0}},\quad \Delta c_{\mathrm{H}} = \max(c_{\mathrm{H}}) - \min(c_{\mathrm{H}}),$$

$$\Delta\overline{c}_S = \frac{\Delta c_S}{c_{T0}},\ \Delta c_S = \max(c_S) - \min(c_S),$$

$$\Delta\overline{m}_K = \frac{\Delta m_K}{m_{K0}},\ \Delta m_K = \max(m_K) - \min(m_K).$$

where c_{T0}, m_{K0} are the time-averaged coaxial rotor thrust and torque coefficients.

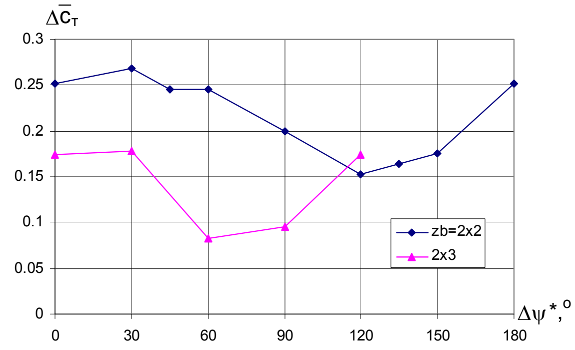

Figure 15.

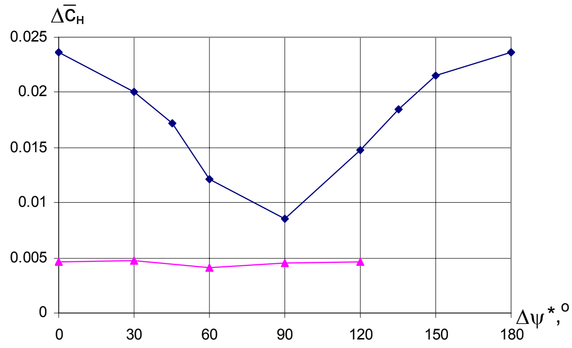

Figure 16.

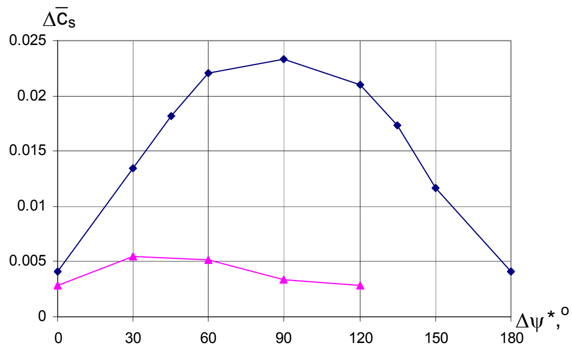

Figure 17.

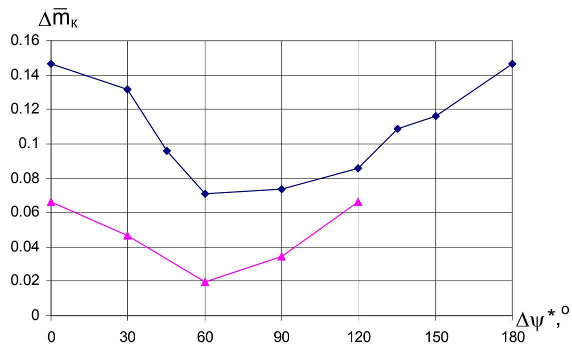

Figure 18.

Increasing number of blades results in reducing amplitude of all the forces and moments.

It is significant that minimum of Δc_S (see Fig. 17) corresponds to $\Delta\psi^*=0$, and decreasing Δc_T, Δc_H и Δm_K by choosing an appropriate phase angle leads to a significant increase in Δc_S.

The minimum value of Δc_T and its corresponding phase angle are considerably determined by induction and blade-vortex interactions. Fig. 19 shows the comparison between thrust coefficients Δc_T of coaxial rotors with two different distances between the higher and the lower rotors: $y/R=0.16$ and $y/R=1$. Increasing distance between the rotors reduces their mutual interaction and minimum Δc_T shifts to $\Delta\psi^*=90°$.

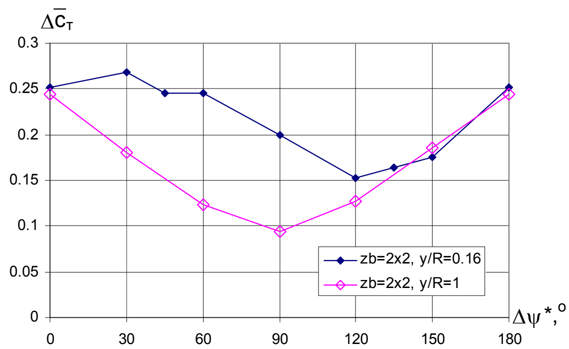

Figure 19.

With an increase in advance ratio up to $\overline{V}$=0.4 (Fig. 20) time-dependent variation of airloads increases. For a rotor with z_b=2×2 the amplitude Δc_T grows by several times as compared with the case of $\overline{V}$=0.2, provided c_{T0} remains constant.

Δc_T reaches its minimum with $\Delta\psi^*$=90° (for z_b=2×2), which can be explained by diminished interaction between the rotors (the same way as for increased distances between the rotors).

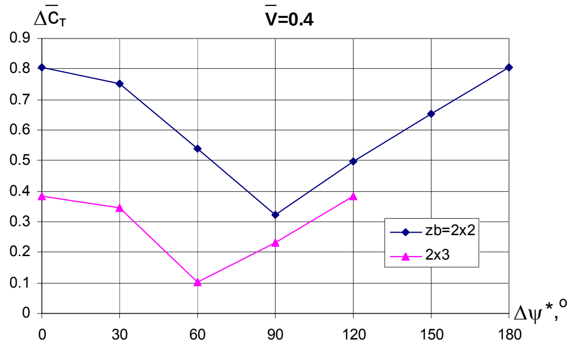

Figure 20.

Thus, an adequate choice of the phase angle allows halving the time-dependent variation of the loads transmitted to the fuselage at $\overline{V}$=0.2. With an increase in advance ratio this value becomes even higher. In addition, $\Delta c_{T\ min}$ largely depends on the number of blades, and its behavior changes with increasing advance ratio (see Fig. 21).

The obtained results demonstrate the necessity of using the transitional free-vortex mathematical model in helicopter rotor system design process, under conditions of various limitations imposed on the rotor design and operational parameters.

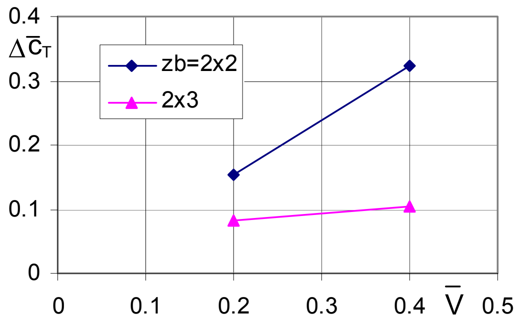

Figure 21.

7 COMPARISON OF CALCULATED AERODYNAMIC COEFFICIENTS OF A ROTOR WITH EXPERIMENTAL RESULTS.

A comparison of calculated and experimental aerodynamic coefficients was carried out for a large-scale model of a rotor in TsAGI T-104 wind tunnel.
The rotor is four bladed, with rectangular blade planform. Diameter D=4m. Blade tip speed ωR=215m/s.

Fig. 22 – 24 show experimental and calculated functions $c_T/\sigma=f(m_K/\sigma)$ and $c_X/\sigma=f(c_T/\sigma)$ in operating conditions corresponding to advance ratios $\overline{V}$=0.26, 0.33, 0.39 and rotor angles of attack α_R=-5°, -10°, -15°. Calculated results show good agreement with the experiment when c_T/σ <0.2. Differences at higher c_T/σ may be explained by blade tip stall, which was not modeled in these computations.

Generally the agreement of calculated and experimental aerodynamic coefficients is acceptable.

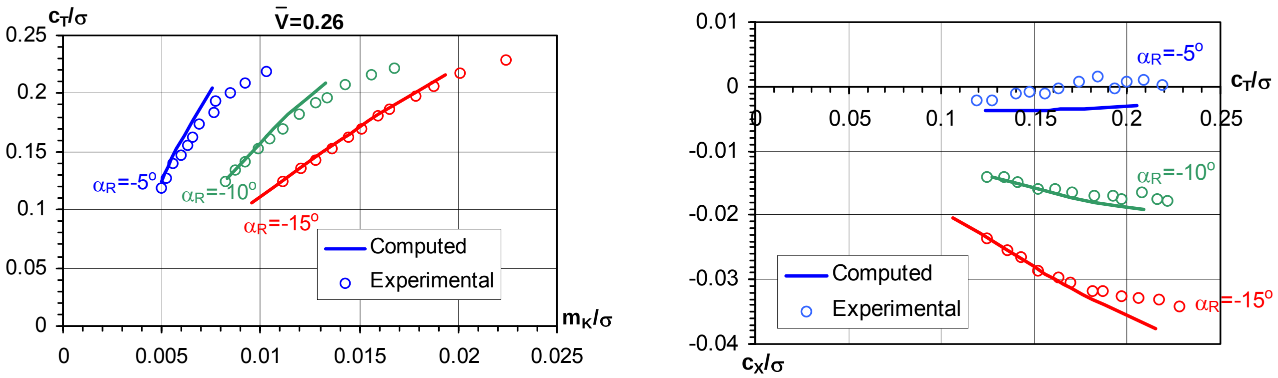

a) b)

Figure 22.

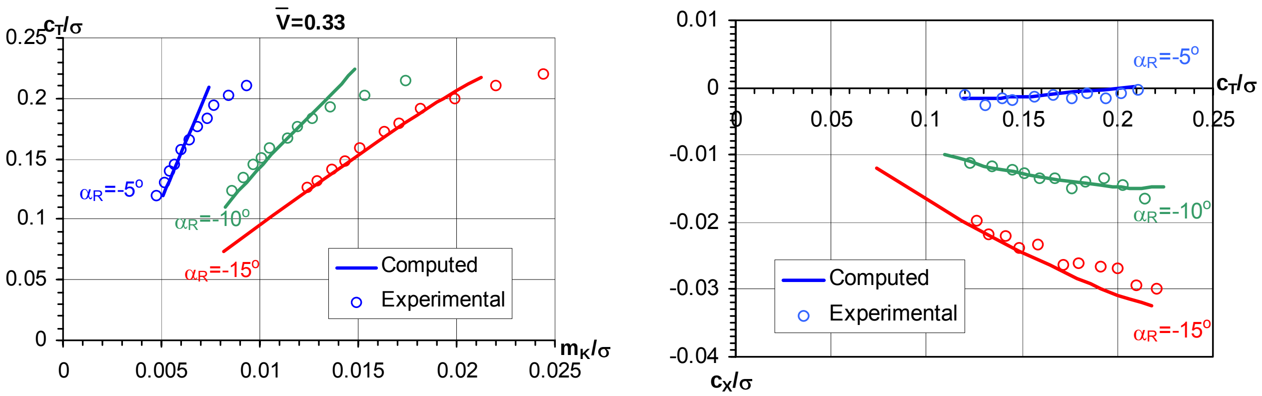

a) b)

Figure 23.

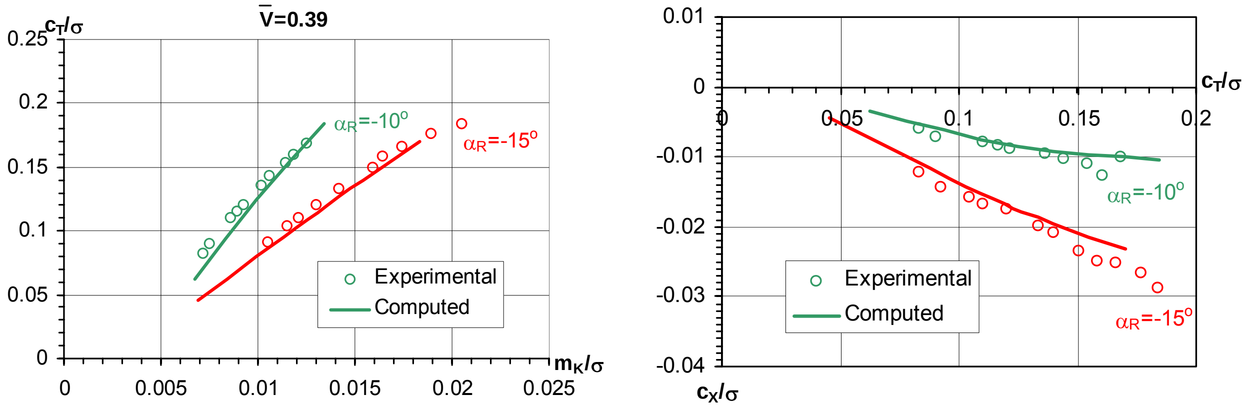

a) b)

Figure 24.

CONCLUSIONS

A new mathematical model of the main rotor (in particular coaxial) is developed. It takes into account the peculiarities of rotor aerodynamics at high flight speed and in maneuver, including induction and vortex interactions, spatial and unsteady nature of the airflow around the blades, separation in the reverse flow region.

The numerical analysis has allowed evaluating influence of the above factors on the aerodynamic coefficients of the main rotor and has proved the developed model to be an effective tool for the main rotor systems design process.

REFERENCES

[1] V.E. Baskin, E.S. Vozhdaev, L.S. Vildgrube, G.I. Maikapar, "Theory of a Rotor", Moscow, 1973.

[2] S.M. Belotserkovsky, B.E. Loktev, M.I. Nisht. "Computer-aided investigation of aerodynamic and aeroelastic characteristics of helicopter rotors", Moscow, 1992.

[3] V. Anikin, D. Kolomenskiy, Yu. Sviridenko, "Simulation of Rotor Aerodynamics at High Flight Speed", 30th European Rotorcraft Forum, Marseilles, 2004.

[4] S.V. Mikheyev, V.A. Anikin, Yu.N. Sviridenko, D.S. Kolomenskiy, "Development directions of the modeling of helicopter main rotor aerodynamic characteristics", Polet (Flight), №6, 2004.

[5] V.A. Golovkin, R.M. Mirgazov, "Inverse hypothesis of flat sections and its application to wing and rotor aerodynamic analysis", Proceedings of the 6th Forum of the Russian Helicopter Society, 2004.

[6] V. Anikin, B. Kritsky, "Multilevel Mathematical Model of Rotorcraft Aerodynamics", 27th European Rotorcraft Forum, Moscow, 2001.